AJNR

Portable Bedside Low-field MRI for Assessment of Ventricular Size

Vinu Mathew, Timothy R. Lim, Akhil Nair, Amy W. Lin, Joel Kosowan, Yingming A. Chen, Aditya Bharatha and Shobhit Mathur

AJNR Am J Neuroradiol published online 22 April 2025
http://www.ajnr.org/content/early/2025/04/22/ajnr.A8811

Published April 22, 2025 as 10.3174/ajnr.A8811

ORIGINAL RESEARCH

Portable Bedside Low-field MRI for Assessment of Ventricular Size

Vinu Mathew, Timothy R. Lim, Akhil Nair, Amy W. Lin, Joel Kosowan, Yingming A. Chen, Aditya Bharatha and Shobhit Mathur

ABSTRACT

BACKGROUND AND PURPOSE: Low-field portable MRI (pMRI) has been shown to be a useful alternative neuroimaging tool in the emergency department (ED) and intensive care unit (ICU), potentially addressing challenges associated with the transport of critically ill patients. We aimed to evaluate the intermodality reliability between low-field pMRI and conventional neuroimaging (CN) for assessment of ventricular size and hydrocephalus.

MATERIALS AND METHODS: This retrospective study included all patients who underwent point-of-care 64mT pMRI at a single tertiary hospital from March 30, 2022 to January 4, 2024, and had a follow-up CN, either CT or MRI, performed within 24 hours of the pMRI scan. Two raters independently evaluated pMRI images for presence of hydrocephalus while blinded to CN. Bifrontal diameter, maximum skull and Evans index were recorded. Interrater and intermodality agreement between pMRI and CN were evaluated by using the intraclass coefficient (ICC) and Cohen's kappa.

RESULTS: Fifty-six patients (mean age of 53.5 (± 14.6) years, 61% male) were included in this study. Hydrocephalus was identified in 12 (21%) on pMRI and 13 (23%) on CN. Interrater agreement on pMRI was almost perfect for bifrontal diameter (ICC 0.94, 95% CI 0.89-0.97), Evans index (ICC 0.92, 95%CI 0.86-0.95) and substantial for determination of hydrocephalus (κ = 0.72), all p <0.01. Intermodality agreement between pMRI and CN was also near perfect for averaged measurements of bifrontal diameter (ICC 0.94, 95% CI 0.88-0.97), Evans index (ICC 0.95, 95%CI 0.92-0.97) and determination of hydrocephalus (κ = 0.95), all p<0.01. Using CN as reference standard, pMRI had sensitivity and specificity of 92% (95% CI 0.85-0.99) and 100% (95% CI 1.0-1.0), respectively on qualitative visual assessment, and 80% (95% CI 0.70-0.90) and 98% (95% CI 0.94-1.0), respectively on quantitative assessment using an Evans index cut off of 0.3.

CONCLUSIONS: Low-field pMRI demonstrated excellent interrater agreement and strong concordance with CN in assessing ventricular size, highlighting its potential as an effective point-of-care tool for neuro-critical care applications.

ABBREVIATIONS: pMRI= portable MRI; CN = conventional neuroimaging; ED= emergency department; ICU= intensive care unit; ICC= intraclass coefficient; pCT= portable CT; TCS = Transcranial Sonography

Received January 3rd,2025 ; accepted after revision April 4th,2025.

From the department of Medical Imaging(V.M,T.R.L,A.W.L, J.K,Y.A.C, A.B,S.M), St. Michael's Hospital, University of Toronto, Toronto, Ontario, Canada; Temerty Faculty of Medicine(A.N), University of Toronto, Toronto, Ontario, Canada; Li Ka Shing Knowledge Institute(A.B, S.M), Toronto, Ontario, Canada

The authors declare no conflicts of interest related to the content of this article.

Please address correspondence to Shobhit Mathur, MD, Department of Medical Imaging, St. Michael's Hospital, 30 Bond Street, Toronto, Ontario, Canada, M5B 1W8; e-mail: Shobhit.Mathur@unityhealth.to.

SUMMARY SECTION

PREVIOUS LITERATURE: Low-field portable MRI (pMRI) can detect acute neurological conditions such as ischemic stroke and intracranial hemorrhage and offers a safe point-of-care alternative to conventional neuroimaging (CN) in emergency departments and intensive care units. One indication for serial imaging is monitoring ventricular size, but studies evaluating the utility of pMRI in comparison to CN remain limited.

KEY FINDINGS: Portable MRI showed almost perfect interrater and intermodality agreement with CN for commonly used measurements of ventricular size, such as bifrontal diameter and Evans index. Using CN as reference standard, pMRI also had high specificity and sensitivity for determination of hydrocephalus, both qualitatively and when using a quantitative Evans Index cut off (0.3).

KNOWLEDGE ADVANCEMENT: Low-field pMRI is a reliable bedside imaging modality for assessing ventricular size and hydrocephalus, with strong intermodality agreement to CN. It advances the potential role of pMRI as an alternative imaging tool to address the challenges associated with transporting neurocritical patients.

Copyright 2025 by American Society of Neuroradiology.

INTRODUCTION

Hydrocephalus is characterized by an abnormal distension of the ventricular system of the brain, either from abnormal production of cerebrospinal fluid (CSF), altered CSF dynamics or obstruction of CSF absorption. Acute hydrocephalus may result as a complication of subarachnoid hemorrhage, intraparenchymal hemorrhage (with or without intraventricular extension), infection, tumors or shunt failure[1,2]. This requires prompt and accurate diagnosis, most commonly with the use of imaging, to guide timely medical or surgical intervention. Conventional imaging pathways entail transport of patients to dedicated imaging suites in the radiology department, which is often time consuming and comes with increased risks of adverse events. The reported rates of adverse events during intrahospital transportation of critically ill patients range from 26% to 79%[3–5]. These include potential hemodynamic instability, dislodgement of life-support equipment, venous access limitations, compromise of monitoring equipment and increased susceptibility to infections[6–8]. Furthermore, patient transport requires coordination of specialized personnel and resources, such as nursing staff, respiratory therapists, and portable monitors, to maintain patient stability during transfer, all of which come with significant financial cost [6,7].

Low-field portable MRI (pMRI) has emerged as an alternative neuroimaging tool to address these logistical and clinical challenges[9]. Studies have shown the capability of pMRI to detect ischemic stroke, intracranial hemorrhage, midline shift, and hypoxic ischemic injury, making it a valuable tool in the emergency department (ED) and intensive care unit (ICU) settings[9–15]. Although it suffers from a lower SNR and resolution compared to conventional fixed high field MRI (1.5T or 3T), pMRI offers the advantage of point-of-care imaging, eliminating the need for patient transport. Furthermore, it requires less stringent environmental controls such as shielding and ferromagnetic restrictions typically associated with conventional MRI. pMRI exams have been safely conducted in environments that contain ferromagnetic material, including ventilators, monitoring devices, and infusion pumps[16].

In this study, we aimed to evaluate the concordance between low-field pMRI and conventional neuroimaging (CN) such as fixed CT scan and high-field strength MRI in the assessment of ventricular size and determination of hydrocephalus.

MATERIALS AND METHODS

This study was done as part of a quality improvement initiative at a single tertiary hospital assessing the utilization of 64mT pMRI system (Swoop, Hyperfine) compared with conventional CT and MRI. This initiative was formally reviewed and approved by institutional authorities and deemed to neither require formal research ethics board approval nor written informed consent from participants. This retrospective analysis included all patients who underwent point-of-care 64mT pMRI and had a follow-up CN (either CT or MRI) within 24 hours of the pMRI scan at the same institute from March 30, 2022, to January 4, 2024. A 24-hour interval was chosen to ensure minimal change in the clinical status of the patient between the pMRI and CN scans. Follow-up CN was performed at the discretion of the referring team based on their clinical judgement, as well as to confirm or further characterize findings seen on pMRI where necessary. Exclusion criteria include significant artifacts on the pMRI images, interval surgery, and patients with significant change in the clinical status between the scans. Four patients were excluded based on these criteria. This study adhered to the methodology proposed by the Standards for Reporting Diagnostic Accuracy (STARD) guidelines, with the relevant completed STARD checklist provided as supplementary material.

Imaging Acquisition and Evaluation

The pMRI examinations were performed using an 8-channel head coil and using the manufacturer's standard parameters. The studies included at least an axial T2 and axial FLAIR sequence with variable addition of axial T1, axial DWI/ADC, as well as coronal and/or sagittal T2 or FLAIR sequence, depending on the clinical indication with sequence parameters for pMRI added to supplementary material.

Two subspecialty-trained radiologists (one each from neuroradiology and emergency radiology), independently measured maximum bifrontal diameter and skull diameter, defined as the maximal internal diameter of the skull at the same level where the bifrontal diameter was obtained (Figure 1). Axial T2 images were preferred for the measurements and axial FLAIR images were used when axial T2 images were not available. Presence and absence of hydrocephalus was determined qualitatively through visual inspection and quantitatively using an Evans index cut off of 0.3[17]. pMRI and CN were evaluated separately. Qualitative visual assessment for hydrocephalus was based on the presence of ballooning of the frontal horns out of proportion to cortical sulcal size, rounding of the temporal horns, and evidence of transependymal edema. No adverse events during the performance of pMRI and CN were recorded.

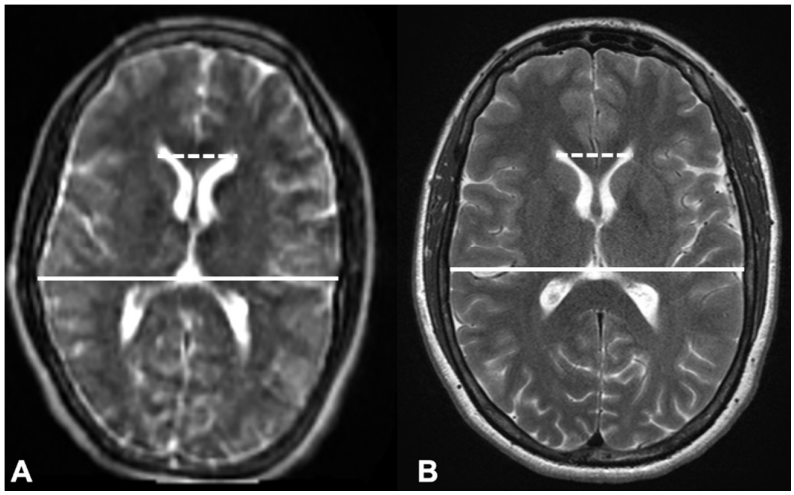

FIG 1. Representative measurements of bifrontal diameter (dotted line) and maximum internal skull diameter (continuous line) on axial T2-weighted pMRI (A) and conventional MRI (B) images.

Statistical Analysis

Test characteristics were computed by using the CN performed soonest after the pMRI as the reference standard. Interrater reliability on pMRI and CN as well as intermodality agreement between the averaged measurements on pMRI and CN were evaluated using Cohen's kappa and Intraclass Correlation Coefficient (ICC). Kappa and ICC values interpreted as follows: <0.20 indicates slight agreement, 0.21–0.40 fair agreement, 0.41–0.60 moderate agreement, 0.61–0.80 substantial agreement, and >0.80 almost perfect agreement[18]. Bland-Altman plots were also generated to visualize the agreement between the raters and between pMRI and CN with calculation of bias and limits of agreement. A significance level of 0.05 was used for all analyses. All statistical analyses were conducted using R studios (version 4.4.2, R Foundation for Statistical Computing, Vienna, Austria).

RESULTS

A total of 56 patients were included in the study (figure 2) of which 34 (60.7%) were male and 22 (39.3%) were female, with mean (± SD) age of 53.5 (± 14.6) years, range 20-78 years. Most of the patients (n=49, 87.5%) were admitted to the ICU, while 4 (7.1%) were ward patients, and 3 (5.4%) were from the ED (Table 1). On qualitative visual analysis, 12 (21.4%) had hydrocephalus on pMRI and 13 (23.2%) on CN. The primary causes of hydrocephalus were intracranial hemorrhage from trauma or aneurysm rupture (n=10) and obstructive hydrocephalus due to posterior fossa masses (n=3). CN was CT in 44 (78.6%) and MRI in 12 (21.4%) patients.

Table 1: Patient Demographics

Demographics	Number
Total patients	56
Mean age	53.5 (±14.6)
Male	34 (60.7%)
Female	22 (39.3%)
ICU patients	49 (87.5%)
Ward Patients	4 (7.1%)
ED patients	3 (5.4%)

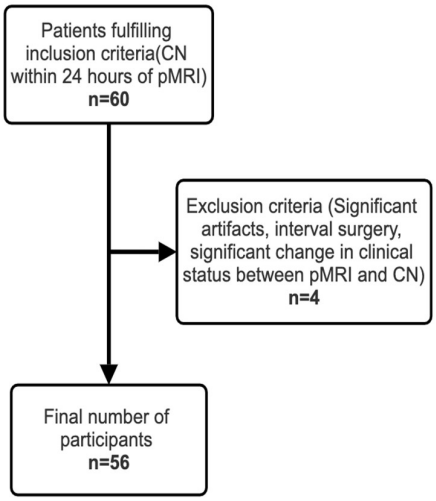

FIG 2. Inclusion-exclusion flow chart.

Interrater Agreement for Measurements of Ventricular Size

The raters had almost perfect agreement for measurement of bifrontal diameter (ICC, 95%CI = 0.94, 0.89-0.97, p<0.01) and Evans index (ICC, 95%CI = 0.92, 0.86-0.95, p<0.01) and substantial agreement for skull diameter (ICC, 95%CI = 0.78, 0.63-0.87, p<0.01) on pMRI. For assessment of presence or absence of hydrocephalus, there was substantial interrater agreement on both qualitative visual evaluation (κ = 0.72) and using a dichotomous Evans index cut-off of 0.3 (κ = 0.71) (Figure 3).

On CN, interrater agreement was also near perfect for bifrontal diameter (ICC, 95%CI = 0.98, 0.96-0.99), skull diameter (ICC, 95%CI = 0.83, 0.72-0.90), and Evans index (ICC, 95%CI = 0.96, 0.94-0.98), all with p-values of <0.01. For determination of hydrocephalus, interrater agreement was almost perfect on both qualitative evaluation (κ = 0.90) and using Evans index (κ = 0.94) (Table 2).

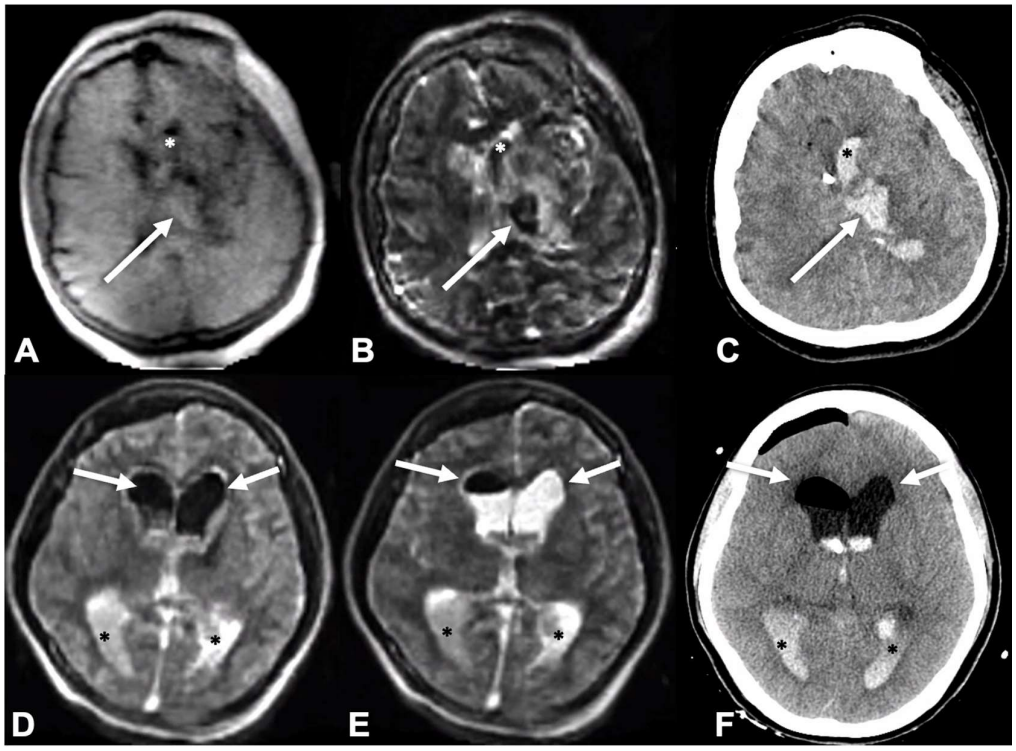

FIG 3. Examples of concordant pMRI and CN findings in patients without and with hydrocephalus. A-C. Axial T1- (A), axial T2-weighted (B) pMRI images and axial CT (C) showing a left thalamocapsular hematoma (arrows) with intraventricular extension (asterisks), but no gross ventricular dilatation. D-F. Ventricular dilatation (arrows) is seen on axial FLAIR (D), axial T2-weighted

(E) and axial CT (F) images in a patient with intraventricular hemorrhage (asterisks). Air within the right frontal convexity and right frontal horn is from extraventricular drain insertion.

Table 2: Interrater and Intermodality Agreement for Bifrontal Diameter, Skull Diameter and Evans Index Measurements and Hydrocephalus.

Parameter	pMRI Interrater Agreement	CN Interrater Agreement	Intermodality Agreement between pMRI and CN
Bifrontal Diameter, ICC (95% CI), p-value	0.94 (0.89-0.97), p<0.01	0.98 (0.96-0.99), p<0.01	0.94 (0.88-0.97), p<0.01
Skull Diameter, ICC (95% CI), p-value	0.78 (0.63-0.87), p<0.01	0.83 (0.72-0.90), p<0.01	0.83 (0.37-0.93), p<0.01
Evans Index, ICC (95% CI), p-value	0.92 (0.86-0.95), p<0.01	0.96 (0.94-0.98), p<0.01	0.95 (0.92-0.97), p<0.01
Hydrocephalus (Qualitative Evaluation), % Agreement, κ	89%, κ=0.72	96%, κ=0.90	98%, κ=0.95
Hydrocephalus (Evans Index > 0.3), % Agreement, κ	91%, κ=0.71	98%, κ=0.94	95%, κ=0.81

pMRI, portable MRI; CN, conventional neuroimaging; ICC, Intraclass correlation coefficient; CI, confidence interval

Intermodality Agreement for Measurements of Ventricular Size

Intermodality agreement was near perfect for the averaged measurements of bifrontal diameter (ICC, 95%CI = 0.94, 0.88-0.97), skull diameter (ICC, 95%CI = 0.83, 0.37-0.93) and Evans index (ICC, 95%CI = 0.95, 0.91-0.97) on pMRI and CN, all with p-values < 0.01 (Table 2). There was also near perfect intermodality agreement for determination of hydrocephalus on both qualitative evaluation (κ = 0.95) and when using an Evans index cut of 0.3 (κ = 0.81) (Table 2). Subgroup analyses were done for patients with and without hydrocephalus, which did not affect the results. For the subgroup without hydrocephalus, intermodality agreement was near perfect for bifrontal diameter (ICC, 95%CI = 0.85, 0.62-0.93), skull diameter (ICC, 95%CI = 0.87, 0.41-0.95) and Evans index (ICC, 95%CI = 0.88, 0.78-0.94) on pMRI and CN, all with p-values < 0.01. For the subgroup with hydrocephalus, intermodality agreement was also near perfect for bifrontal diameter (ICC, 95%CI = 0.95, 0.85-0.99), and Evans index (ICC, 95%CI = 0.95, 0.84-0.98) on pMRI and CN, all with p-values < 0.01; however, there was poor intermodality agreement for skull diameter (ICC, 95%CI = 0.33 (-0.48-0.75), p=0.18.

On Bland-Altman plot analysis (Figure 4), the mean differences for bifrontal diameter measurements on CN and pMRI was -0.136 mm (limit of agreement [LOA]: -0.79 mm to 0.52 mm). For skull diameter, mean difference was -0.316 mm (LOA: -1.2 mm to 0.57 mm). For Evans index, mean difference was minimal at 0.004 mm (LOA: -0.05 mm to 0.05 mm). These results indicate strong intermodality agreement, with pMRI closely aligning with CN across all parameters and observers.

Considering CN as reference standard, pMRI had high sensitivity and specificity for determining presence of hydrocephalus on qualitative visual assessment (92% [95% CI: 0.85-0.99] and (100% [95% CI:1.0-1.0], respectively) and using the set Evans index threshold (80% [95% CI: 0.70-0.90] and 98% [95%CI: 0.94-1.0], respectively) (Table 3).

Table 3: Test Characteristics of pMRI for Hydrocephalus using Conventional Neuroimaging as reference

Parameter	Sensitivity (95% CI)	Specificity (95% CI)	PPV (95% CI)	NPV (95% CI)
Hydrocephalus (Qualitative Evaluation)	92% (0.85-0.99)	100% (1.0-1.0)	100% (1.0-1.0)	98% (0.94-1.0)
Hydrocephalus (Evans Index > 0.3)	80% (0.70-0.90)	98% (0.94-1.0)	89% (0.81-0.97)	96% (0.90-1.0)

CI, confidence interval; PPV, positive predictive value; NPV, negative predictive value

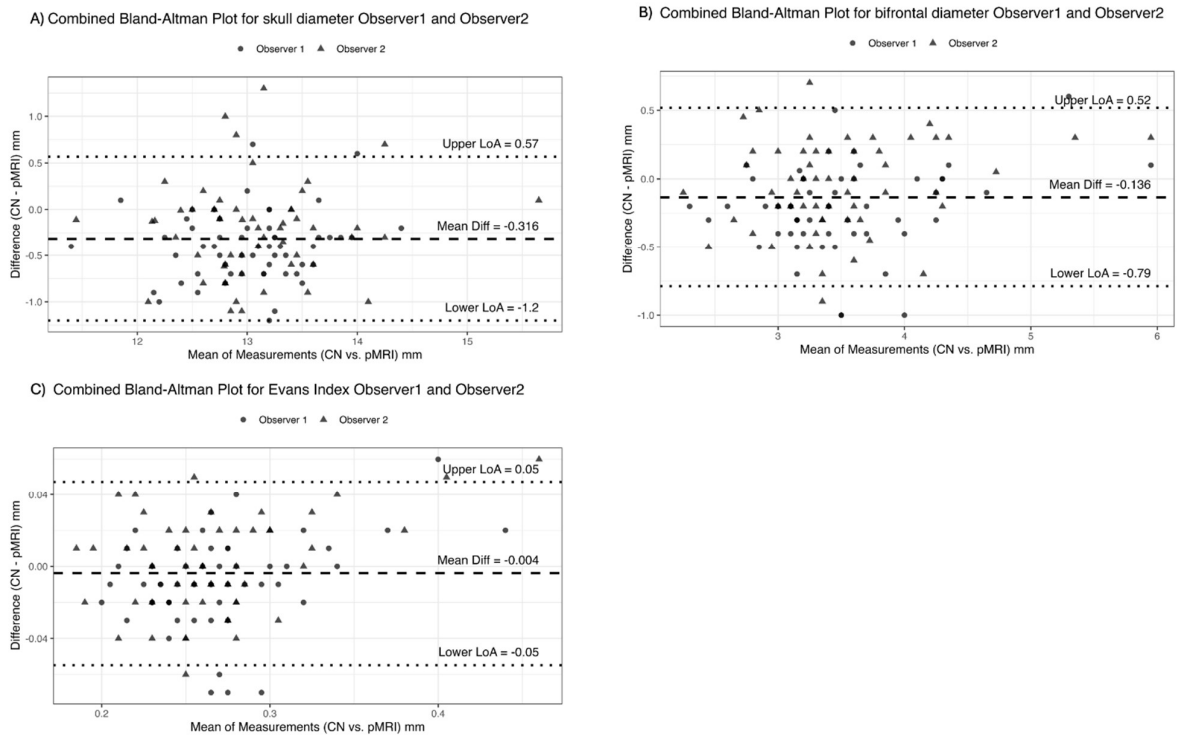

FIG 4. Bland-Altman Plots of portable MRI and conventional neuroimaging measurements.

DISCUSSION

The potential applications of pMRI continue to expand, providing the advantage of bedside imaging that eliminates the need for patient transport—a challenging and potentially risky process for critically ill patients. In this study, we demonstrated significant interrater agreement for pMRI and substantial intermodality agreement between pMRI and CN in evaluating ventriculomegaly and commonly used ventricular size metrics, such as bifrontal diameter and Evans index. Bland-Altman analysis shows no significant bias.

Neuroimaging is vital in neurocritical care. Non-contrast CT remains the preferred imaging modality for acute neurological conditions due to its speed, accessibility, and minimal screening requirements[19]. Frequent imaging helps monitor neurologic deterioration, assess progression of mass effect, manage hydrocephalus and ventricular drains, and screen for clinically occult hydrocephalus which may be difficult in unconscious or sedated ICU patients[20,21]. However, transporting unstable patients for CN pose significant risks[3].

Low-field pMRI has emerged as a safe and feasible neuroimaging alternative when transporting patients for diagnostic imaging is contraindicated[9,16]. Although small lesions may not be detected due to technical limitations, pMRI has been proven effective for bedside evaluation of intracranial hemorrhages[12,13], ischemic infarcts[11,22], hypoxic-ischemic injury following cardiac arrest[15], leukoaraiosis[23], and even demyelinating lesions[24,25]. Studies have also reported significant intermodality concordance between pMRI and CN for assessing midline shifts[14], hematoma volumes[12] and optic chiasm decompression after transsphenoidal resection of sellar-suprasellar mass lesions[26]. Recently, Velagapudi et al. demonstrated excellent agreement between pMRI and conventional MRI for estimating ventricular volumes in pediatric patients, with a minor mean increase of 2% observed on pMRI[27]. Similarly, our study showed strong agreement between pMRI and CN in assessing ventricular size in adult patients. We evaluated bifrontal diameter and Evans index rather than using segmentation methods, measurements commonly applied and directly translatable to clinical practice. While our study population included a relatively small proportion of patients with hydrocephalus, our primary objective was to assess the reliability and concordance of pMRI in measuring ventricular size. Despite the sample size limitation, intermodality agreement remained high, and pMRI correctly identified all but one case of hydrocephalus diagnosed on CN. These findings suggest that pMRI is a reliable tool for evaluating ventricular size, even in patients with varying degrees of ventricular enlargement.

Other bedside tools such as portable CT (pCT) scanners and transcranial sonography (TCS), are available but have inherent limitations. pCT produces images with lower spatial resolution and signal-to-noise ratio than fixed CT, while exposing patients to radiation and requiring specialized personnel and lead shielding[28–31]. TCS, provides limited visualization of intracranial structures, restricted to evaluating the third ventricle and perimesencephalic region[32,33]. In contrast, low-field pMRI involves no ionizing radiation, does not require specialized radiation technologists, supports multiple imaging sequences (including diffusion-weighted imaging), and allows unrestricted access to the clinical environment during acquisition. The device's low magnetic field strength ensures safe entry of hospital staff and patients, without requiring the removal of ferromagnetic objects essential for clinical care[16]. Furthermore, a retrospective semiquantitative descriptive analysis also showed that using pMRI for select indications in the ICU, including hydrocephalus and ventricular drain

placements, could potentially allow additional patients to undergo fixed CN[34].

The primary limitation of this study is its single-center, retrospective design and relatively small patient cohort, which may introduce selection and recall biases. Additionally, pMRI and CN were not conducted simultaneously. Given that ventricular size can fluctuate over a short span of time, this timing discrepancy could potentially affect the concordance between pMRI and conventional measurements. However, we minimized this issue by ensuring a maximum interval of 24 hours between scans and confirming that patients experienced no significant clinical changes during this period. We did not perform a separate analysis comparing pMRI performance in acute uncompensated hydrocephalus (with periventricular edema) versus compensated hydrocephalus due to limited sample size and retrospective data. While our results demonstrate excellent reliability and concordance, we acknowledge inherent limitations of low-field MRI, including reduced spatial resolution and lower signal-to-noise ratio compared to conventional imaging. These limitations are consistent with findings reported in a recent systematic review evaluating the diagnostic performance of low-field MRI across clinical applications[35].

CONCLUSIONS

Low-field pMRI had excellent interrater agreement and high concordance with CN for assessment of ventricular size, making it a useful point-of-care tool for this indication in neuro-critical care.

REFERENCES

1. Kartal MG, Algin O. Evaluation of hydrocephalus and other cerebrospinal fluid disorders with MRI: An update. *Insights Imaging* 2014;5:531–41.
2. Chahlavi A, El-Babaa SK, Luciano MG. Adult-onset hydrocephalus. *Neurosurg Clin N Am* 2001;12:753–60, ix.
3. Murata M, Nakagawa N, Kawasaki T, et al. Adverse events during intrahospital transport of critically ill patients: A systematic review and meta-analysis. *The American Journal of Emergency Medicine* 2022;52:13–9.
4. Parmentier-Decrucq E, Poissy J, Favory R, et al. Adverse events during intrahospital transport of critically ill patients: incidence and risk factors. *Ann Intensive Care* 2013;3:10.
5. Jia L, Wang H, Gao Y, et al. High incidence of adverse events during intra-hospital transport of critically ill patients and new related risk factors: a prospective, multicenter study in China. *Crit Care* 2016;20:12.
6. McLean B, Thompson D. MRI and the Critical Care Patient: Clinical, Operational, and Financial Challenges. Plackett T, ed. *Critical Care Research and Practice* 2023;2023:1–8.
7. Fanara B, Manzon C, Barbot O, et al. Recommendations for the intra-hospital transport of critically ill patients. *Crit Care* 2010;14:R87.
8. Veiga VC, Postalli NF, Alvarisa TK, et al. Adverse events during intrahospital transport of critically ill patients in a large hospital. *Revista Brasileira de Terapia Intensiva* 2019;31.
9. Sheth KN, Mazurek MH, Yuen MM, et al. Assessment of Brain Injury Using Portable, Low-Field Magnetic Resonance Imaging at the Bedside of Critically Ill Patients. *JAMA Neurol* 2021;78:41.
10. Kuoy E, Glavis-Bloom J, Hovis G, et al. Point-of-Care Brain MRI: Preliminary Results from a Single-Center Retrospective Study. *Radiology* 2022;305:666–71.
11. Yuen MM, Prabhat AM, Mazurek MH, et al. Portable, low-field magnetic resonance imaging enables highly accessible and dynamic bedside evaluation of ischemic stroke. *Sci Adv* 2022;8:eabm3952.
12. Mazurek MH, Cahn BA, Yuen MM, et al. Portable, bedside, low-field magnetic resonance imaging for evaluation of intracerebral hemorrhage. *Nat Commun* 2021;12:5119.
13. Mazurek MH, Parasuram NR, Peng TJ, et al. Detection of Intracerebral Hemorrhage Using Low-Field, Portable Magnetic Resonance Imaging in Patients With Stroke. *Stroke* 2023;54:2832–41.
14. Sheth KN, Yuen MM, Mazurek MH, et al. Bedside detection of intracranial midline shift using portable magnetic resonance imaging. *Sci Rep* 2022;12:67.
15. Beekman R, Crawford A, Mazurek MH, et al. Bedside monitoring of hypoxic ischemic brain injury using low-field, portable brain magnetic resonance imaging after cardiac arrest. *Resuscitation* 2022;176:150–8.
16. Prabhat AM, Crawford AL, Mazurek MH, et al. Methodology for Low-Field, Portable Magnetic Resonance Neuroimaging at the Bedside. *Front Neurol* 2021;12:760321.
17. Zhou X, Xia J. Application of Evans Index in Normal Pressure Hydrocephalus Patients: A Mini Review. *Front Aging Neurosci* 2022;13:783092.
18. Fleiss JL, Cohen J. The Equivalence of Weighted Kappa and the Intraclass Correlation Coefficient as Measures of Reliability. *Educational and Psychological Measurement* 1973;33:613–9.
19. Williamson C, Morgan L, Klein J. Imaging in Neurocritical Care Practice. *Semin Respir Crit Care Med* 2017;38:840–52.
20. Fried HI, Nathan BR, Rowe AS, et al. The Insertion and Management of External Ventricular Drains: An Evidence-Based Consensus Statement : A Statement for Healthcare Professionals from the Neurocritical Care Society. *Neurocrit Care* 2016;24:61–81.
21. Oddo M, Crippa IA, Mehta S, et al. Optimizing sedation in patients with acute brain injury. *Crit Care* 2016;20:128.
22. Sujijantarat N, Koo AB, Jambor I, et al. Low-Field Portable Magnetic Resonance Imaging for Post-Thrombectomy Assessment of Ongoing Brain Injury. *SVIN* 2023;3:e000921.
23. De Havenon A, Parasuram NR, Crawford AL, et al. Identification of White Matter Hyperintensities in Routine Emergency Department Visits Using Portable Bedside Magnetic Resonance Imaging. *JAHA* 2023;12:e029242.
24. Arnold TC, Tu D, Okar SV, et al. Sensitivity of portable low-field magnetic resonance imaging for multiple sclerosis lesions. *NeuroImage: Clinical* 2022;35:103101.
25. Lim TR, Suthiphosuwan S, Micieli J, et al. Low-Field (64 mT) Portable MRI for Rapid Point-of-Care Diagnosis of Dissemination in Space in Patients Presenting with Optic Neuritis. *AJNR Am J Neuroradiol* 2024;45:1819–25.
26. Hong CS, Lamsam LA, Yadlapalli V, et al. Portable MRI to assess optic chiasm decompression after endoscopic endonasal resection of sellar and

suprasellar lesions. *Journal of Neurosurgery* https://doi.org/10.3171/2023.5.JNS23174.
27. Velagapudi V, Artz NS, Fite JK, et al. Low-Field Portable MR Imaging to Evaluate Ventricular Volumes: A Single-Center Retrospective Study. *AJNR Am J Neuroradiol* 2024;45:1076–80.
28. Butler WE, Piaggio CM, Constantinou C, et al. A mobile computed tomographic scanner with intraoperative and intensive care unit applications. *Neurosurgery* 1998;42:1304–10; discussion 1310-1311.
29. Matson MB, Jarosz JM, Gallacher D, et al. Evaluation of head examinations produced with a mobile CT unit. *The British Journal of Radiology* 1999;72:631–6.
30. Gunnarsson T, Theodorsson A, Karlsson P, et al. Mobile computerized tomography scanning in the neurosurgery intensive care unit: increase in patient safety and reduction of staff workload. *Journal of Neurosurgery* 2000;93:432–6.
31. LaRovere KL, Brett MS, Tasker RC, et al. Head Computed Tomography Scanning During Pediatric Neurocritical Care: Diagnostic Yield and the Utility of Portable Studies. *Neurocrit Care* 2012;16:251–7.
32. Najjar A, Denault AY, Bojanowski MW. Bedside transcranial sonography monitoring in a patient with hydrocephalus post subarachnoid hemorrhage. *Crit Ultrasound J* 2017;9:17.
33. Widehem R, Bory P, Greco F, et al. Transcranial sonographic assessment of the third ventricle in neuro-ICU patients to detect hydrocephalus: a diagnostic reliability pilot study. *Ann Intensive Care* 2021;11:69.
34. Islam O, Lin AW, Bharatha A. Potential application of ultra-low field portable MRI in the ICU to improve CT and MRI access in Canadian hospitals: a multi-center retrospective analysis. *Front Neurol* 2023;14:1220091.
35. Mašková B, Rožánek M, Gajdoš O, et al. Assessment of the Diagnostic Efficacy of Low-Field Magnetic Resonance Imaging: A Systematic Review. Diagnostics. 2024;14(14):1564.

SUPPLEMENTAL FILES

Supplemental Table 1: STARD Checklist Portable MRI vs. Conventional Neuroimaging for Ventricular Size Assessment

Section & Topic	No	Item	Completed
TITLE OR ABSTRACT			
	1	Identification as a study of diagnostic accuracy using at least one measure of accuracy (such as sensitivity, specificity, predictive values, or AUC)	Yes
ABSTRACT			
	2	Structured summary of study design, methods, results, and conclusions (for specific guidance, see STARD for Abstracts)	Yes
INTRODUCTION			
	3	Scientific and clinical background, including the intended use and clinical role of the index test	Yes
	4	Study objectives and hypotheses	Yes
METHODS			
Study design	**5**	Whether data collection was planned before the index test and reference standard were performed (prospective study) or after (retrospective study)	Yes
Participants	**6**	Eligibility criteria	Yes
	7	On what basis potentially eligible participants were identified (such as symptoms, results from previous tests, inclusion in registry)	Yes
	8	Where and when potentially eligible participants were identified (setting, location and dates)	Yes
	9	Whether participants formed a consecutive, random or convenience series	Yes
Test methods	**10a**	Index test, in sufficient detail to allow replication	Yes
	10b	Reference standard, in sufficient detail to allow replication	Yes
	11	Rationale for choosing the reference standard (if alternatives exist)	Yes
	12a	Definition of and rationale for test positivity cut-offs or result categories of the index test, distinguishing pre-specified from exploratory	Yes
	12b	Definition of and rationale for test positivity cut-offs or result categories of the reference standard, distinguishing pre-specified from exploratory	Yes
	13a	Whether clinical information and reference standard results were available to the performers/readers of the index test	Yes
	13b	Whether clinical information and index test results were available to the assessors of the reference standard	Yes
Analysis	**14**	Methods for estimating or comparing measures of diagnostic accuracy	Yes
	15	How indeterminate index test or reference standard results were handled	Yes
	16	How missing data on the index test and reference standard were handled	N/A
	17	Any analyses of variability in diagnostic accuracy, distinguishing pre-specified from exploratory	N/A

	18	Intended sample size and how it was determined	N/A
RESULTS			
Participants	**19**	Flow of participants, using a diagram	Yes
	20	Baseline demographic and clinical characteristics of participants	Yes
	21a	Distribution of severity of disease in those with the target condition	Yes
	21b	Distribution of alternative diagnoses in those without the target condition	Yes
	22	Time interval and any clinical interventions between index test and reference standard	Yes
Test results	**23**	Cross tabulation of the index test results (or their distribution) by the results of the reference standard	Yes
	24	Estimates of diagnostic accuracy and their precision (such as 95% confidence intervals)	Yes
	25	Any adverse events from performing the index test or the reference standard	Yes
DISCUSSION			
	26	Study limitations, including sources of potential bias, statistical uncertainty, and generalisability	Yes
	27	Implications for practice, including the intended use and clinical role of the index test	Yes
OTHER INFORMATION			
	28	Registration number and name of registry	N/A
	29	Where the full study protocol can be accessed	N/A
	30	Sources of funding and other support; role of funders	Yes

Table 2: Sequence Parameters for Hyperfine Portable MRI

Sequence	T2	FLAIR	T1	DWI (b-value= 900s/mm2)
TE/TR (ms)	161/1600	170/3000	5.4/880	62/850
TI (ms)	-	1290	322	-
Receiver bandwidth (kHz)	64	64	64	52
Echo train length	64	68	32	44
Navigator	1	1	1	4
FA (excitation/refocusing)	90/180	90/180	90/180	90/180
FA (inversion)	-	180	-	-
Resolution (mm)	1.5 × 1.5 × 5	1.7 × 1.7 × 5	1.6 × 1.6 × 5	2.4 × 2.4 × 6
Scan Time (min:sec)	5:20	7:50	4:00	8:40

TE = echo time; TR = repetition time; TI = inversion time; DWI = diffusion-weighted imaging; FA = flip angle; FLAIR = fluid-attenuated inversion recovery.